

The impact of transmission power levels set size on lifetime of wireless sensor networks in smart grids

Hüseyin Uğur YILDIZ^{1*} 

Department of Electrical and Electronics Engineering, Faculty of Engineering, TED University, Ankara, Turkey

Received: 29.03.2018

Accepted/Published Online: 20.10.2018

Final Version: 29.11.2018

Abstract: Wireless sensor networks (WSNs) have been confirmed as one of the most promising technologies for many smart grid (SG) applications due to their low complexity and inexpensive costs. A typical WSN is formed with numerous battery limited sensor nodes mounted on critical components of a SG system for monitoring applications. Acquired monitoring data by sensor nodes are conveyed to the base station generally by using multihop communication techniques. WSN-based SG applications encounter severe propagation losses due to extreme channel conditions of the SG environment. In order to reduce possible packet errors caused by channel variations, transmission power control approaches can be adopted where the set size of available transmission power levels differs among the utilized hardware platforms. Usage of low transmission power levels can reduce the energy dissipation of nodes, which may lead to high packet drops. On the other hand, usage of high transmission power levels can prevent packet errors. Nonetheless, this alternative solution may lead to premature death of sensor nodes. Depending on the networking conditions, it is possible to confront applications such that the utilization of all available power levels provided by the node hardware may be unnecessary. In order to overcome this issue, determination of optimal transmission power levels set size for WSN-based SG applications becomes a critical research topic to prolong the network lifetime. In this work, we propose an optimization model to maximize the network lifetime while limiting the size of the transmission power levels set. Furthermore, we propose two strategies that are built on top of the optimization model to investigate the impact of the most used and optimal power levels on WSN lifetime considering several SG environments under various networking conditions.

Key words: Smart grids, wireless sensor networks, optimization, network lifetime, power levels set size

1. Introduction

For many years, power grid systems were monitored and maintained through expensive wired communication principles [1]. In recent years, power grid systems are diagnosed by using wireless communication techniques in order to reduce high expenditure costs of wired communications [2, 3]. One of the most suitable wireless communication technologies used in power distribution systems is called the wireless sensor network (WSN). WSNs are constructed with numerous battery limited inexpensive sensor nodes and a base station, where the data acquired by sensor nodes are transmitted to the base station either by using single-hop or commonly multihop communication techniques. Usage of modern communication technologies such as WSNs in traditional power grid systems for monitoring, automation, and control purposes creates the paradigm of smart grids (SGs) [4]. Limited battery power of sensor nodes poses a great challenge for long-term monitoring in SG applications.

*Correspondence: hugur.yildiz@tedu.edu.tr

WSN-based SG systems are subject to severe propagation losses due to the electromagnetic interference generated in the SG infrastructure [5, 6]. In order to reduce packet errors due to severe propagation losses, transmission power control (TPC) approaches can be adopted. The idea behind TPC approaches is to adjust the transmission power levels from a set of available discrete transmission power levels [7] for achieving a reliable communications performance. TPC techniques can be categorized as network-level (i.e. a global transmission power level is employed throughout the network) and link-level (i.e. each link can adjust its transmission power level locally) [8].

The size (cardinality) of the transmission power levels set depends on the WSN node hardware used in SG systems. One of the most popular WSN node platforms used in SG systems is the Tmote Sky platform [9]¹. This node hardware uses the Chipcon CC2420 radio module, which has 31 different transmission power levels. Another popular node platform is Mica2, which uses a Chipcon CC1000 radio module having 26 different transmission power levels [7]. Regardless of the node platform that is used, packet errors can be mitigated by utilizing the maximum available transmission power level. This approach has a drawback of energy efficiency such that nodes consume excessive amounts of energy for transmission, which would yield low lifetimes. To attain energy efficiency, less amounts of energy can be consumed by the nodes if lower transmission power levels are utilized; however, in this way the chance of packet drops increases. Hence, there is a trade-off of utilizing transmission power levels to attain the energy efficiency and prolong the network lifetime. On the other hand, depending on the networking area, the usage of transmission power levels may vary greatly. When the network size is small, propagation losses tend to be lower when compared to larger network sizes. In this case, there is a tendency of using lower transmission power levels. As the network size increases, propagation losses increase, which would result in usage of higher transmission power levels to avoid packet errors. In these possible scenarios, some of the available transmission power levels (depending on the node platform that is used in SG systems) may be unused. Thus, determination of optimal transmission power levels plays a vital role in lifetime elongation when designing distributed protocols for WSNs in SGs.

In this work, we develop an optimization model by using the mixed integer linear programming (MILP) framework that maximizes the network lifetime. By using this optimization model, two strategies are proposed to determine the most used and optimal transmission power levels sets for WSN-based SG applications. We enumerate our original contributions as follows:

1. We develop a MILP model that maximizes the network lifetime while limiting the size of the transmission power level set. The proposed MILP model employs a detailed handshaking-based link-layer energy dissipation model, which utilizes a link-level TPC approach. Moreover, the link-layer model uses the energy consumption characteristics of Tmote Sky node platforms and an experimental path loss model (i.e. log-normal shadowing) considering the path loss parameters for several SG environments described in [1].
2. We propose a strategy, which is built onto the aforementioned MILP model, called the histogram-based power levels decision (HB-PLD) strategy that determines the most used transmission power levels for a maximized lifetime according to the transmission power level usage statistics for six SG environments considering various network sizes without limiting the size of the transmission power levels set. Furthermore, we gradually reduce the cardinality of the most used transmission power levels set and investigate the impact of this approach on the network lifetime quantitatively.

¹Tmote Sky datasheet: http://www.snm.ethz.ch/snmwiki/pub/uploads/Projects/tmote_sky_datasheet.pdf

3. We also propose another strategy called optimization-based power levels decision (OB-PLD), which determines the optimal transmission power levels that maximize the network lifetime while limiting the size of the transmission power levels set.
4. We numerically compare lifetime and solution time differences between HB-PLD and OB-PLD strategies for various network densities and several SG environments.

The rest of the paper is organized as follows. We present the related work on the determination of optimal transmission power level sets for wireless networks and especially WSNs in Section 2. Our system model including the wireless channel model, link-layer energy consumption model, optimization framework, and proposed strategies is described in Section 3. The results of the numerical analysis are provided in Section 4. Conclusions are presented in Section 5.

2. Related work

In the literature, there has been a great interest in transmission power level selection approaches for wireless networks in the last two decades [10–19]. Moreover, there is a growing body of work in the literature on this research topic for WSNs. We present an overview of the related work in the following paragraphs.

In [10], a single channel ALOHA protocol was considered and its throughput was investigated under full-load conditions by considering both exponential back-off retransmission method and capture effects. Packets are transmitted with various power levels where the set size of power levels is in the interval of 1–10. In [11], the authors developed an algorithm to determine the optimal set of transmission powers in each link for mobile networks, which use directional antennas deployed in a hostile environment. The proposed method avoids interceptions by adversaries with minimum probability. The set size of transmission power levels in each directional bin is given in the interval of 1–4. In [12], an adaptive M -ary quadrature amplitude modulation (M-QAM) system was considered for throughput maximization. The proposed system uses a small number of power levels (i.e. 2 to 3) and code rates. It was shown that the proposed system can achieve high throughput like continuous adaptive systems in slow fading environments. Another work was performed for M-QAM systems to identify optimal delay constrained rate and power adaptation for type-I hybrid automatic repeat request (ARQ) scheme over fading channels by using a Markov decision process in [13]. The proposed method uses a discrete power level in each time slot, which is selected from a predetermined transmission power level set. In [14], the transmission power was modeled as a function of packet collisions and selection of power levels was investigated in large-scale ALOHA networks in a decentralized manner. In that work, the authors considered a finite transmission power levels set such that the transmission power level is increased with a power step (which can be either small or large) until the packet transmission within the defined interval is successful. Properly chosen larger power steps are shown to have higher throughput when compared to small power steps, which yield a decline in throughput when the network load is high. In [15], an adaptive transmission power scheme for flat-fading wireless channels was developed. The proposed transmission mechanism is based on a set of finite power levels per code. The authors concluded that using 4 codes and 4 power levels per code resulted in an average spectral efficiency within 1 dB of the continuous-rate continuous-power Shannon capacity. In [16], a cognitive radio system was considered where the secondary users vary their transmission powers depending on the information contained in the spectrum sensor. Peak power and average interference constraints are enforced at the secondary and primary users, respectively. The authors revealed that if any transmission is occurring, only the peak power level is utilized. In [17], effects of TPC on interference for wireless mesh networks on a real

testbed were investigated. The transmission power levels set has a cardinality of 6 and contains power levels between 7 dBm and 19 dBm with a step size of 2 dBm. In that work, the power level for each testbed was determined, which avoids interference while keeping each link's robustness. In [18], an algorithm was proposed to determine optimal power levels that minimize the total transmission power for each retransmission period for a hybrid ARQ method used in quasi-static Rayleigh fading channels. In [19], an analytical model by using randomized transmission power for throughput maximization in IEEE 802.11 networks was developed. The proposed solution determines the attempt probability of a randomly selected node as well as obtaining the optimal probability mass function of transmission powers to maximize the network throughput. In that work, only 5 transmission power levels were considered.

The literature on the selection of transmission power levels in WSNs is growing day-to-day [7, 20–28]. In [20], the authors proposed a distributed power controlled contention-based medium access control (MAC) layer protocol for WSNs. The authors considered a radio module that has 8 distinct power levels between 0.05 mW and 25 mW. In [21], an analytical framework was proposed to evaluate the advantages of using variable transmission power levels in WSNs for geographical routing. In that work, the set size of available transmission power levels was defined in the interval of 1–4. The authors of [22] and [23] investigated link channel characteristics in wireless body area sensor networks. Among these works, Natarajan et al. [22] used three predetermined power level sets (i.e. –25 dBm, –15 dBm, and –10 dBm) for the analysis. On the other hand, Lee et al. [23] used all available power levels for CC2420 radios. In [24], the joint impact of packet length and transmission power level on the energy consumption between two WSN nodes using CC1000 radios was investigated. In that work, the authors adopted 26 transmission power levels of CC1000 radios. In [25], discrete TPC and rate adaption algorithms were proposed for ultrareliable machine-to-machine control applications, in which a finite set of transmit rates is only supported with cardinality 4 and 8. In [26], two topology control techniques (i.e. depth adjustment and TPC) for geographic routing in underwater WSNs were studied. In that work, all underwater nodes are identical and the set size of transmission power levels is 7. In [27], a discrete TPC scheme was developed for Poisson-clustered ad hoc networks where each transmitter can use predetermined discrete transmission power levels. In [28], total power consumption in the network was minimized while guaranteeing strong connectivity between node pairs in the network. Sensor nodes are allowed to use only 2 power levels. In our previous work [7], we focused on determining optimal transmission power levels set for conventional terrestrial WSNs, which maximizes the network lifetime. Twenty-six different power levels of CC1000 radios were employed in that work. Our results revealed that the drop in maximum network lifetime is observed to be at most 5% if the set size of transmission power levels is reduced to 13 from 26.

In summary, in the literature on determining the optimal transmission power levels set, some works aimed to maximize the throughput of the network [10, 12–14, 16, 19, 27], while some others focused on the minimization of the energy consumption in the network [18, 20, 21, 24, 26, 28]. There are also several studies considering other important performance metrics such as link quality [17, 22, 23], concurrent transmission time [25], average spectral density [15], and accuracy of localization [11]. Moreover, there are only a few works that determined optimal transmission power levels set by using a real WSN node platform (such as CC1000 and CC2420) [7, 22–24]. To the best of our knowledge, there are no controlled studies that investigate the impacts of determining transmission power levels that maximize the network lifetime by using an actual WSN node platform quantitatively for SG applications. In order to fill this gap in the literature, in this study, we develop an optimization model to determine the most used and optimal transmission power levels sets for WSN-

based SG applications with the objective of maximization of network lifetime by using the power consumption characteristics of a real WSN node platform.

3. System model

In the following subsections, we present our channel model (in Section 3.1), link-layer energy dissipation model (in Section 3.2), developed optimization method for lifetime maximization (in Section 3.3), and proposed strategies (in Section 3.4). Throughout this work, we use Tmote Sky mote platforms to construct the WSN, which is used for SG applications.

3.1. Wireless channel model

We model the wireless channel as a log-normal shadowing channel to calculate the propagation loss. In this respect, the signal-to-noise ratio (i.e. $\overline{\gamma_{ij}}(l)$ in dBm) at receiving node j due to the transmission from node i with power level l can be calculated as:

$$\overline{\gamma_{ij}}(l) = \underbrace{\overline{P_{tx}^{ant}}(l) - \overline{PL_0} + 10n\log_{10}\left(\frac{d_{ij}}{d_0}\right) - \overline{X_\sigma} - \overline{P_n}}_{\overline{P_{rx,ji}^{ant}}(l)}, \quad (1)$$

where $\overline{P_{tx}^{ant}}(l)$ is the antenna transmit power with transmission power level l (given in dBm), $\overline{P_{rx,ji}^{ant}}(l)$ is the reception power (given in dBm), $\overline{PL_0} = 55$ dB is the reference path loss value [29], n is the path loss exponent, d_{ij} is the distance of a link (in meters), d_0 is the reference distance (in meters), $\overline{X_\sigma} \sim \mathcal{N}(0, \sigma^2)$ is used to model the shadowing and is a Gaussian random variable with mean zero and variance σ^2 (in dB), and $\overline{P_n}$ is the noise floor.

We consider three different SG environments, which are the Outdoor 500 KV Substation (i.e. Out), Underground Network Transformer Vault (i.e. Und), and Indoor Main Power Room (i.e. In). We also consider two different propagation characteristics, namely line-of-sight (LOS) and non-line-of-sight (NLOS). Path loss exponents, shadowing variables, and noise floor values are determined with field tests conducted at Georgia Power, Atlanta, GA, USA [1] and are listed in Table 1.

There are eight reported $P_{tx}^{ant}(l)$ values (i.e. for power levels 3, 7, 11, 15, 19, 23, 27, and 31) available for Chipcon CC2420 radios, which are used in Tmote Sky nodes. In order to accurately determine the optimal transmission power levels set, we perform a curve-fitting method to approximately determine all 31 available power levels for CC2420 radios in Figure 1a. Moreover, circuitry transmission power consumption values (i.e. $P_{tx}^{crc}(l)$) for this radio platform are given in Figure 1b [9].

Tmote Sky platforms use offset quadrature phase shift keying as the modulation scheme. The successful L bits of data packet reception probability at node j due to the transmission of node i with power level l after including processing gain costs (i.e. $\eta = 16$ [9]) can be calculated as:

$$p_{ij}^{s,L}(l) = \left(1 - Q\left(\sqrt{\eta \times \gamma_{ij}(l)}\right)\right)^L, \quad (2)$$

where $\gamma_{ij}(l)$ is the signal-to-noise ratio, which is given in ordinary form. $p_{ij}^{f,L}(l) = 1 - p_{ij}^{s,L}(l)$ shows the failure reception probability.

Table 1. Empirically obtained path loss exponents (n), standard deviations (σ – dB) of the shadowing random variable, and noise floors ($\overline{P_n}$ – dBm) for six SG environments [1].

Environment	Abbreviation	n	σ	$\overline{P_n}$
Outdoor 500 KV Substation–LOS	OutLOS	2.42	3.12	–93
Outdoor 500 KV Substation–NLOS	OutNLOS	3.51	2.95	–93
Indoor Main Power Room–LOS	InLOS	1.64	3.29	–92
Indoor Main Power Room–NLOS	InNLOS	2.38	2.25	–92
Underground Network Transformer Vault–LOS	UndLOS	1.45	2.45	–88
Underground Network Transformer Vault–NLOS	UndNLOS	3.15	3.19	–88

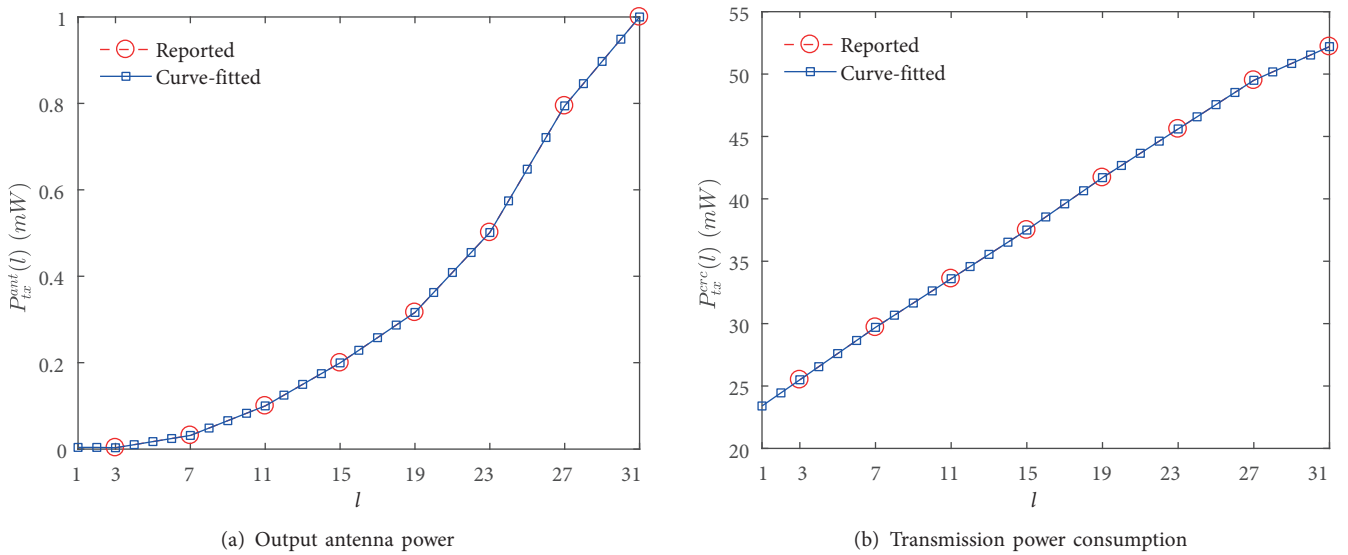


Figure 1. Output antenna power ($P_{tx}^{ant}(l)$ – mW) and power consumption for transmission ($P_{tx}^{erc}(l)$ – mW) as a function of power levels (l) for the CC2420 radio platform.

3.2. Link-layer energy dissipation model

We model our link-layer by using a slotted communication scheme such that a single slot consists of durations for M_P byte of data packet transmission (i.e. $T_{tx}(M_P)$), M_A byte of acknowledgment (ACK) packet transmission (i.e. $T_{tx}(M_A)$), propagation delay (i.e. T_{pd}), and guard times (i.e. $2 \times T_{grd}$), which are applied at both the beginning and end of the active slot to prevent synchronization errors [9]. We take $M_P = 128$ bytes, $M_A = 12$ bytes, and the data rate of Tmote Sky platforms (R) as 250 kbps [9]. Thus, we can calculate the active slot time as $T_{slot} = [2 \times T_{grd} + T_{tx}(M_P) + T_{pd} + T_{tx}(M_A)] = 4.78$ ms.

A two-way handshaking policy is applied during an active slot to ensure a reliable communication. Handshaking is considered successful if both the M_P byte and M_A byte of data and ACK packets are successfully received at the intended nodes. Hence, we can calculate the probability of a successful handshake as $p_{ij}^{s,HS}(l) = p_{ij}^{s,M_P}(l) \times p_{ji}^{s,M_A}(l)$. Considering a stop-and-wait ARQ scheme, the expected retransmission rate is obtained as $\lambda_{ij}^l = \frac{1}{p_{ij}^{s,HS}(l)}$.

3.2.1. Transmitter energy consumption model

Transmission of the M_P byte of a data packet costs $P_{tx}^{crc}(l) \times T_{tx}(M_P)$ J of energy at the transmitter node. After transmission of the M_P byte of a data packet, the transmitter nodes stays in receive/idle mode for $T_{slot} - T_{tx}(M_P)$ s in order to receive an ACK packet. During this period, $P_{rx}^{crc} \times (T_{slot} - T_{tx}(M_P))$ J of energy are dissipated. In this notation, $P_{rx}^{crc} = 69$ mW is the power consumption for reception [9]. Packet processing energy is dissipated only once during a single slot, which costs $E_{PP} = 12.66$ μ J of energy [9]. When considering retransmissions with the factor of λ_{ij}^l , overall energy consumption of transmitter node i can be expressed as:

$$E_{ij,tx}^l = E_{PP} + \lambda_{ij}^l \times [P_{tx}^{crc}(l) \times T_{tx}(M_P) + P_{rx}^{crc} \times (T_{slot} - T_{tx}(M_P))]. \quad (3)$$

3.2.2. Receiver energy consumption model

The receiver node waits $T_{slot} - T_{tx}(M_A)$ s to receive a data packet from the transmitter node i , which costs $P_{rx}^{crc} \times [T_{slot} - T_{tx}(M_A)]$ J of energy. As soon as the data packet is received, node j uses transmission power level l to transmit an ACK packet back to node i , in which $P_{tx}^{crc}(l) \times T_{tx}(M_A)$ J of energy is dissipated. We define ε to denote the amount of energy consumed for data reception and ACK transmission during a successful handshake. If the handshaking has failed due to the ACK packet errors in the reverse path, we need to repeat the whole handshaking, which costs extra energy dissipation with a factor of $\frac{p_{ij}^{s,MP}(l) \times p_{ji}^{f,MA}(l)}{p_{ij}^{s,HS}(l)}$ due to the retransmissions. Furthermore, if the data packet is dropped in the forward link, the receiver node would stay in receive/idle mode for the whole slot duration, in which $\frac{p_{ij}^{f,MP}(l)}{p_{ij}^{s,HS}(l)} \times [P_{rx}^{crc} \times T_{slot}]$ J of energy is dissipated while considering retransmissions. Thus, the total energy consumption of the receiving node j in a single slot (with packet processing costs) is obtained as:

$$E_{ji,rx}^l = \overbrace{P_{rx}^{crc}[T_{slot} - T_{tx}(M_A)] + [P_{tx}^{crc}(l) \times T_{tx}(M_A)]}^{\varepsilon} + \frac{p_{ij}^{s,MP}(l)p_{ji}^{f,MA}(l)}{p_{ij}^{s,HS}(l)}\varepsilon + \frac{p_{ij}^{f,MP}(l)}{p_{ij}^{s,HS}(l)}(P_{rx}^{crc} \times T_{slot}) + E_{PP}. \quad (4)$$

3.3. Optimization model

In this part, we model our optimization problem by using the MILP technique, which maximizes the network lifetime (i.e. N , in terms of rounds) while limiting the size of the transmission power levels set. The network lifetime is defined as the time elapsed until the first node depletes its battery energy [30]. In terms of seconds, the network lifetime is calculated as $N \times T_r$, where $T_r = 10$ s is assumed to be the round duration. We define sets V and W to stand for the set of all nodes (including the base station) and all sensor nodes (excluding the base station), respectively. The set E is used to represent all directed edges (links). The set of transmission power levels is defined as \mathcal{L} . The decision variable of the optimization model is the amount of data packets (size of 128 bytes) using power level l traversing from node i to node j , which is denoted by f_{ij}^l . The optimization model with its constraints is given in Figure 2.

In Eq. (5), incoming flows, generated flows at each round (i.e. $N \times s_i$), and outgoing flows are balanced at each sensor node i . Total active time for sensor node i (i.e. T_{act}^i) consists of durations for transmission, reception, and acquiring data including retransmissions, which is calculated in Eq. (6). Note that $T_{DA} = 5$ ms is the time to acquire a data packet, which is dissipated once per round [9]. In Eq. (7), energy required for

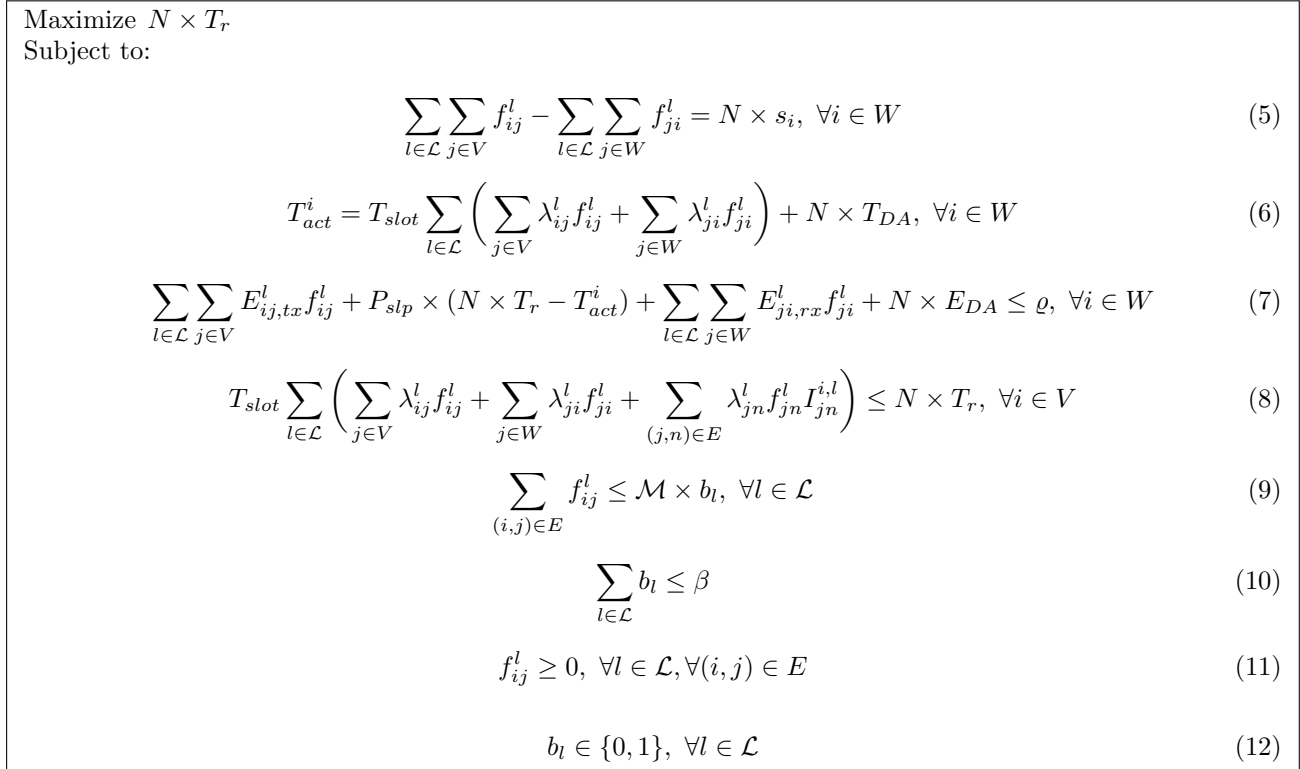


Figure 2. The optimization model to maximize network lifetime while limiting the size of the transmission power levels set.

transmission, reception, sleep, and data acquisition at each sensor node i is limited to the initial battery of each node (i.e. $\varrho = 25$ kJ). In this constraint, $E_{DA} = 57 \mu\text{J}$ is the energy consumed for data acquisition and $P_{slp} = 3 \mu\text{W}$ is the sleep power [9]. Eq. (8) is used for each node i to limit the aggregated duration of incoming, outgoing, and interfering flows to the total network lifetime in seconds. Interference function at node i (i.e. $I_{jn}^{i,l}$) takes the value of 1 if node i can hear the transmission between node j and node n (i.e. $\overline{P_{rx,ji}^{ant,l}} \geq \overline{P_{sns}}$ or $\overline{P_{rx,ni}^{ant,l}} \geq \overline{P_{sns}}$ where $\overline{P_{sns}} = -94$ dBm is the nominal receiver sensitivity for the Tmote Sky mote platforms). We define the binary decision variable b_l to denote whether transmission power level l is used (i.e. $b_l = 1$) or not (i.e. $b_l = 0$). By using b_l , in Eq. (9), we prohibit the flows using power level l within the network if $b_l = 0$. In Eq. (10) the set size of the transmission power levels is limited to β (which is a constant). Finally, Eqs. (11) and (12) show the boundaries of the decision variables used in the optimization model.

3.4. Proposed strategies

In this part, we present the principles of our proposed strategies that are used to determine the most used (in Section 3.4.1) and optimal transmission power levels (in Section 3.4.2) sets for lifetime maximization in WSN-based SG applications. Note that both methodologies use the base optimization framework given in Figure 2.

3.4.1. Histogram-based power levels decision (HB-PLD) strategy

In the HB-PLD strategy, we first determine the most used transmission power levels for a given WSN topology and SG environment without enforcing any constraints on the set size of the transmission power levels (hence all available power levels can freely be utilized). For this purpose, we solve the optimization problem in Figure 2 without constraints given in Eqs. (9), (10), and (12). According to the optimal flows obtained by solving the optimization model (i.e. f_{ij}^l), a histogram of power levels utilization is prepared. By using the prepared histogram, most utilized power levels are sorted in descending order and corresponding b_l values are marked as 1 (note that the binary variable, b_l , is treated as a parameter). In order to investigate the impact of most used transmission power levels set size on the network lifetime, we reactive the constraints in Eqs. (9), (10), and (12). Then we set β to 16 (only the most used 16 power levels can be utilized) and set parameter b_l as 1 for the most used 16 power levels to observe the changes that occur in the network lifetime. This process continues as β is lowered to 8, 4, 2, and 1.

3.4.2. Optimization-based power levels decision (OB-PLD) strategy

In the OB-PLD strategy, determination of optimal transmission power levels is performed by the optimization model given in Figure 2 instead of a histogram-based approach as stated in the previous part. Different from the HB-PLD strategy, b_l is considered as a binary variable and all constraints presented in Figure 2 are active.

The optimization model given in Figure 2 decides whether power level l is used or not by using the binary variable, b_l . For example, if $b_1 = 1$, then power level 1 is utilized and vice versa. If power level l cannot be utilized (i.e. $b_l = 0$), according to the constraint of Eq. (9), $\sum_{(i,j) \in E} f_{ij}^l \leq 0$. Since $f_{ij}^l \geq 0$ by Eq. (11), there will be no data traffic traversing in the network by using power level l (i.e. f_{ij}^l values are forced to be equal to 0 $\forall (i,j) \in E$). On the other hand, if power level l is used, then $\sum_{(i,j) \in E} f_{ij}^l \leq \mathcal{M}$ according to Eq. (9). This inequality states that the amount of data packets using power level l flowing through all links are bounded to a very large number, \mathcal{M} . In this way, f_{ij}^l values can take positive values. By summing all b_l values, the set sizes of the transmission power levels are determined since b_l values can only be either 0 or 1. In the OB-PLD strategy, the optimization model given in Figure 2 aims to determine the optimal values of b_l that maximizes the network lifetime while satisfying the set size of the transmission power levels constraint (i.e. $\sum_{l \in \mathcal{L}} b_l \leq \beta$). In this notation, β is the upper bound of the set size of the transmission power levels. For example, if $\beta = 8$ (i.e. at most 8 power levels can be utilized), then at most eight b_l values can be 1. Indeed, the optimization model determines which power level will be used for lifetime maximization by setting appropriate b_l values to be 1. As in the HB-PLD strategy, we change β values as 31, 16, 8, 4, 2, and 1, respectively, in order to characterize the effects of β on network lifetime.

4. Analysis

In this part we perform analysis to determine the most used and optimal transmission power levels set sizes and investigate their impacts on network lifetime. The WSN topology is modeled as a disk with radius R_{net} and 39 sensor nodes are randomly distributed within the disk, obeying a uniform distribution. The base station is centered at the disk.

We choose three R_{net} values to model a good, a mediocre, and a bad channel condition for each SG propagation environment such that average successful handshaking probabilities of all links and power levels

Table 2. Network radii (i.e. R_{net}) in meters and corresponding average successful handshake probabilities (i.e. $E[p_{HS}^s]$) for six SG environments.

$E[p_{HS}^s]$	Network radii for six SG environments (in meters)					
	OutLOS	OutNLOS	InLOS	InNLOS	UndLOS	UndNLOS
0.80	10	5	10	5	25	5
0.50	25	10	50	20	200	10
0.25	50	20	120	30	400	20

(i.e. $E[p_{HS}^s] = \frac{\sum_{l \in \mathcal{L}} \sum_{(i,j) \in E} p_{ij}^{s,HS}(l)}{|\mathcal{E}| \times |\mathcal{L}|}$) are approximately 0.80, 0.50, and 0.25. The chosen R_{net} values are reported in Table 2. The wireless channel model (Section 3.1) and the link-layer energy dissipation model (Section 3.2) are developed in MATLAB². Proposed strategies (Section 3.4) are modeled and solved with the General Algebraic Modeling System (GAMS)³.

In this work, a stable communication channel is employed on each link such that path loss values do not change over network lifetime. In the following figures, we present the average values of 50 independent runs where at each run both topology and path loss values for each link are regenerated. Since path loss values vary greatly in each scenario, variations in the channel conditions have already been considered in our work. Nevertheless, in [31] it was shown that channel conditions for WSNs can be accurately estimated with very low overhead. We assume that the base station has the knowledge of topology as in [8]. Since the base station in a typical WSN has higher computational capacity and larger battery power than ordinary nodes, path loss calculations and other necessary decision making actions related to the optimization (data flow planning via optimization, routing, etc.) are performed at the base station in a centralized manner.

We present the cumulative percentage of power levels utilization, which maximizes the network lifetime when there are no restrictions on the set size of transmission power levels (i.e. $\beta = 31$) for OutLOS in Figure 3a, InLOS in Figure 3b, UndLOS in Figure 3c, OutNLOS in Figure 3d, InNLOS in Figure 3e, and UndNLOS in Figure 3f, respectively. In each subfigure, three R_{net} values are used (see Table 2) for each environment. Each subfigure is obtained by solving the HB-PLD strategy and creating a histogram of the power level utilization by inspecting the l index of f_{ij}^l values for 50 different network topologies. It is also important to note that the HB-PLD and OB-PLD strategies yield exactly the same results when there are no restrictions on the cardinality of transmission power levels set. The reason behind this is the constraints given in Eqs. (9), (10), and (12) in the OB-PLD strategy such that these constraints have already been satisfied when $\beta = 31$. Thus, these constraints can be classified as redundant constraints and consecutively the OB-PLD strategy converges to the HB-PLD strategy.

Regardless of the environment, we see that for a dense network (i.e. small R_{net} values) at least 88% of the links utilize power levels less than or equal to 8. As the network size increases, the network gets sparser and hence the utilization percentage of higher power levels increases to reduce the packet errors. When we consider a moderately dense network (i.e. mediocre R_{net} values), the utilization of power levels greatly varies such that we observe that at least 90% of the links utilize transmission power levels less than 26. When the network density is very low (i.e. high R_{net} values), at least 78% of the links utilize power levels except for the highest

²<https://www.mathworks.com/products/matlab.html>

³<https://www.gams.com/>

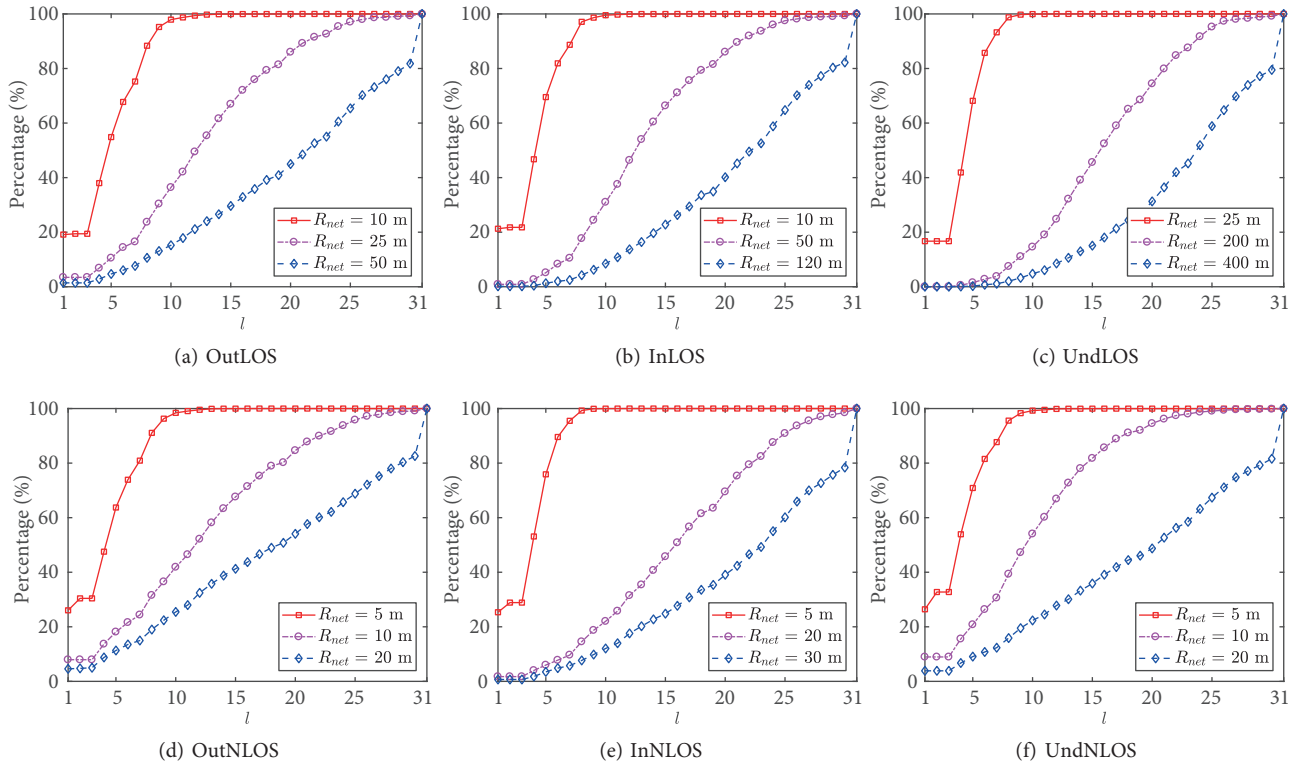


Figure 3. Cumulative percentage of power level utilization for HB-PLD strategy considering six SG environments with three R_{net} values for each environment when $\beta = 31$.

power level (i.e. $l = 31$). This means that at most 22% of the links utilize the highest transmission power level. According to these data, we can infer that it is important to carefully choose transmission power levels according to the network conditions for network lifetime maximization. The reported eight power levels for Tmote Sky motes using Chipcon CC2420 radios (i.e. $l = 3, 7, 11, 15, 19, 23, 27,$ and 31) may give misleading results for accurately estimating the network lifetime. Note that for denser networks low power levels (e.g., power levels 3 to 7) are likely to be used, while for sparse networks high power levels (e.g., power levels 30 and 31) tend to be utilized. Overall, these results indicate that utilization of all available power levels is unnecessary.

We present network lifetimes of the proposed strategies for OutLOS in Figure 4a, InLOS in Figure 4b, UndLOS in Figure 4c, OutNLOS in Figure 4d, InNLOS in Figure 4e, and UndNLOS in Figure 4f, respectively. In each subplot, one SG environment is considered and six curves are presented, which correspond to the results of the HB-PLD and OB-PLD strategies with three R_{net} values for each strategy. In each curve, normalized lifetimes are presented with respect to the cardinality of the optimum transmission power levels set (i.e. β) in order to investigate the relative impact of limiting the size of transmission power levels set on network lifetime. Note that β values are given in descending order for the sake of visualization. Normalized lifetimes are obtained by dividing each lifetime value obtained with a specific β by the lifetime, which is obtained without any constraints on the size of the transmission power levels set (i.e. $\beta = 31$).

For both HB-PLD and OB-PLD strategies, normalized lifetimes decrease as β decreases. Normalized lifetimes can be as low as 0.11 and as high as 0.62 for the HB-PLD strategy (OutNLOS environment with $\beta = 1$ and $R_{net} = 10$ m & 20 m, respectively). As shown in Figure 3d, when $R_{net} = 10$ m, the most used power

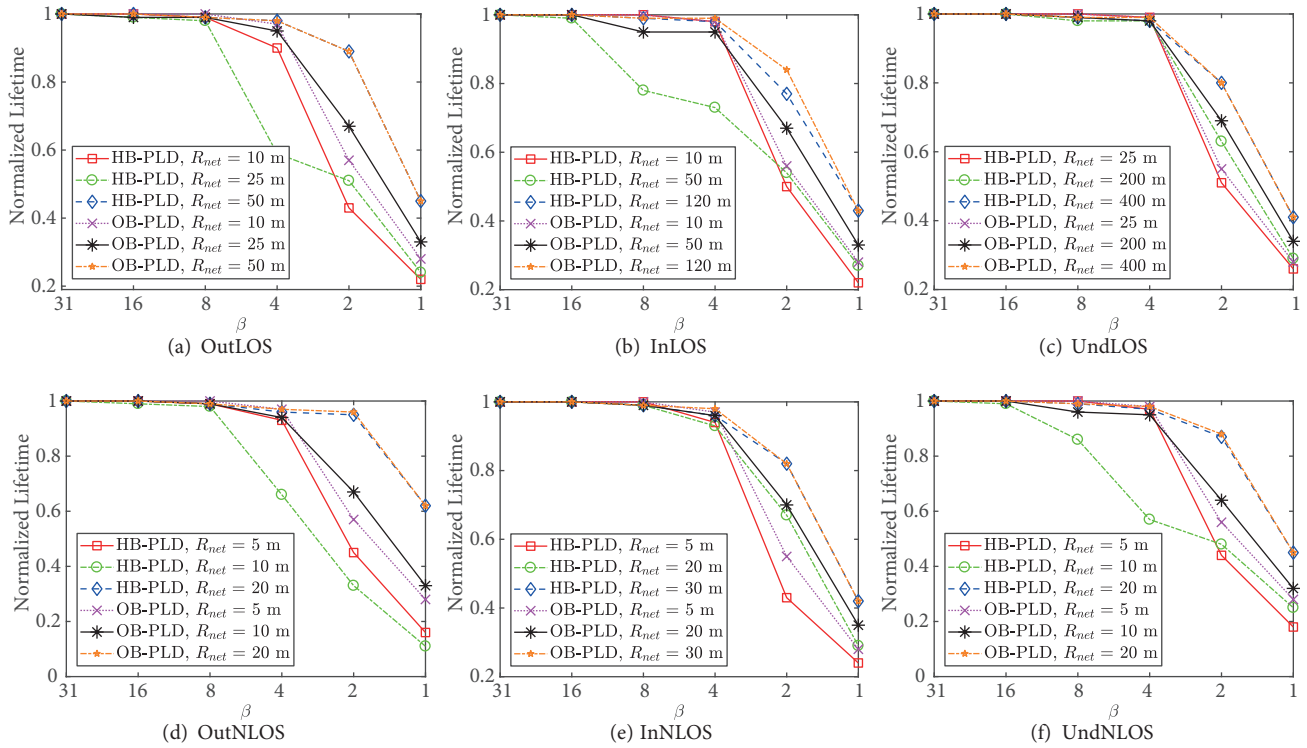


Figure 4. Normalized network lifetimes for HB-PLD and OB-PLD strategies as a function of β for six SG environments and three R_{net} values for each environment.

level is the minimum transmission power level (i.e. $l = 1$) such that around 8% of the links utilize this power level. Hence, when $\beta = 1$, the HB-PLD strategy enforces all links to utilize the minimum transmission power level. Since the utilization of minimum transmission power level leads to more packet errors that incur extra retransmissions, more energy is consumed, which reduces the network lifetime drastically. On the other hand, as the network gets sparser (i.e. $R_{net} = 20$ m), the most utilized power level is the maximum transmission power level, which is used for around 17% of the links. In this case, the $\beta = 1$ constraint employs all links to utilize power level 31, which would reduce the packet errors; thus, extra energy dissipation due to the retransmissions is mostly mitigated, yielding fewer drops in maximum lifetime. Similar interpretations are also valid for other SG environments. Setting the set size of transmission power levels to 16 would lead at most to 1% drop in maximum network lifetime for the HB-PLD strategy. Nevertheless, for $\beta \leq 8$ sparser networks have the highest normalized lifetime values. This result may be explained by the fact that the variation of power levels used for sparse networks is less since higher power levels are preferred for reliable communications when the network size is large.

As stated before, HB-PLD and OB-PLD lifetimes are exactly the same when all available transmission power levels can be utilized. HB-PLD and OB-PLD lifetimes are also same when $\beta = 1$ and the network is sparse due to the fact of utilization of the highest power level as stated in the previous paragraph. When the size of the power levels set is halved (i.e. $\beta = 16$), we observe that OB-PLD lifetimes are at most 0.68% higher than HB-PLD lifetimes. As β decreases, the OB-PLD strategy yields better lifetimes. For example, OB-PLD lifetimes are at most 22.05%, 68.67%, 101.85%, and 199.53% higher than HB-PLD lifetimes for $\beta = 8, 4, 2,$ and $1,$ respectively. These results are related to suboptimal behavior of the HB-PLD strategy. For

the OutNLOS environment with $R_{net} = 10$ m, we stated that the most common power level utilized is the minimum transmission power level. When $\beta = 1$, the HB-PLD strategy enforces links to use $l = 1$. However, the OB-PLD strategy tries to utilize the optimum power level for this configuration, which is obtained as the highest transmission power level. This is the reason why OB-PLD lifetimes can be 199.53% higher than HB-PLD lifetimes. Nevertheless, normalized lifetimes for the OB-PLD strategy can be as low as 0.28 and as high as 0.62. If the set size of transmission power levels is chosen as 4, the drop in maximum lifetime is observed to be between 1% and 6%.

The solution times for the OB-PLD strategy are generally higher than the solution times for the HB-PLD strategy due to b_l . Note that, in the HB-PLD strategy, b_l is defined as a parameter. On the other hand, in the OB-PLD strategy, b_l is a binary variable that naturally increases the solution times for the OB-PLD strategy. Moreover, solution times for the OB-PLD strategy greatly increase as β decreases since the constraint defined in Eq. (10) becomes tighter as β decreases. The computations are performed on a computer with 2.30 GHz Intel Core i5-6200U processor and 8 GB of RAM. Our analysis reveals that solution times are in the intervals of 5.53–29.30 s and 6.86–40.48 s for HB-PLD and OB-PLD strategies, respectively.

5. Conclusion

In this work, two strategies are proposed (i.e. HB-PLD and OB-PLD) to determine the most used and optimal transmission power levels sets for lifetime maximization in WSN-based SGs. The proposed strategies are formulated by using an MILP framework, which is built on top of a detailed link-layer energy dissipation model with an empirically verified channel model. Quantitative analysis is performed on a disk-shaped WSN such that nodes are randomly deployed for six SG environments.

Our main conclusions are as follows:

1. The set size of transmission power levels is small for either dense or sparse networks. For dense/sparse networks lower/higher transmission power levels are utilized. On the other hand, if a network is moderately dense, the set size of transmission power levels gets larger due to the variations of power level utilization on links.
2. Utilization of all available power levels is unnecessary regardless of the network topology and the SG environment. Our analysis shows that using only 16 power levels out of 31 power levels would lead to a maximum lifetime drop of at most 1%.
3. Although the implementation of the HB-PLD strategy is relatively easy due to the treatment of the binary variable as a parameter, determination of transmission power levels set size by using this strategy can greatly underestimate the network lifetime when compared to the OB-PLD strategy if the set size of transmission power levels is planned to be small. Indeed, OB-PLD lifetimes are at most 2 times greater than those of the HB-PLD strategy if a single global power level is planned to be used throughout all links in the network.
4. The HB-PLD strategy can be used with insignificant lifetime deterioration (at most 1% drop) if the half of the available power levels are used. However, as the set size of transmission power levels is lessened, the OB-PLD strategy should be employed for lifetime maximization.
5. Using only 4 transmission power levels in the OB-PLD strategy results in maximum lifetime drop between 1% and 6% regardless of the network size and channel conditions. For this set size, the drop in maximum

network lifetime would be at most 43% if the HB-PLD strategy is employed. This result is useful for designing distributed protocols focused on transmission power control where the burden of utilization of all power levels can greatly be eased by using our proposed solution if the network conditions are unknown.

References

- [1] Güngör VÇ, Lu B, Hancke GP. Opportunities and challenges of wireless sensor networks in smart grid. *IEEE T Ind Electron* 2010; 57: 3557-3564.
- [2] Parikh PP, Kanabar MG, Sidhu TS. Opportunities and challenges of wireless communication technologies for smart grid applications. In: *IEEE PES General Meeting*; 25–29 July 2010; Providence, RI, USA. New York, NY, USA: IEEE. pp. 1-7.
- [3] Şahin D, Güngör VÇ, Koçak T, Tuna G. Quality-of-service differentiation in single-path and multi-path routing for wireless sensor network-based smart grid applications. *Ad Hoc Netw* 2014; 22: 43-60.
- [4] Saputro N, Akkaya K, Uludağ S. A survey of routing protocols for smart grid communications. *Comput Netw* 2012; 56: 2742-2771.
- [5] Gao J, Xiao Y, Liu J, Liang W, Chen CLP. A survey of communication/networking in smart grids. *Future Gener Comput Syst* 2012; 28: 391-404.
- [6] Fadel E, Güngör VÇ, Nassef L, Akkari N, Malik MGA, Almasri S, Akyıldız IF. A survey on wireless sensor networks for smart grid. *Comput Commun* 2015; 71: 22-33.
- [7] Tantur Ç, Yıldız HU, Kurt S, Tavlı B. Optimal transmission power level sets for lifetime maximization in wireless sensor networks. In: *IEEE SENSORS*; 30 October–3 November 2016; Orlando, FL, USA. New York, NY, USA: IEEE. pp. 1-3.
- [8] Yıldız HU, Tavlı B, Yanıkömeroğlu H. Transmission power control for link-level handshaking in wireless sensor networks. *IEEE Sens J* 2016; 16: 561-576.
- [9] Kurt S, Yıldız HU, Yiğit M, Tavlı B, Güngör VÇ. Packet size optimization in wireless sensor networks for smart grid applications. *IEEE T Ind Electron* 2017; 64: 2392-2401.
- [10] Hossain AZME, Sarker JH. On throughput performance of single and multichannel S-ALOHA with exponential backoff retransmission schemes for packet transmissions in multiple power levels. In: *IEEE International Conference on Personal Wireless Communications*; 17–19 December 1997; Mumbai, India. New York, NY, USA: IEEE. pp. 152-156.
- [11] Liu TY, Scholtz RA. An optimal link power set for a mobile communication network with directive/adaptive antennas. In: *MILCOM 97 Proceedings*; 3–5 November 1997; Monterey, CA, USA. New York, NY, USA: IEEE. pp. 782-786.
- [12] Lin L, Yates RD, Spasojevic, P. Adaptive transmission with discrete code rates and power levels. *IEEE T Commun* 2003; 51: 2115-2125.
- [13] Karmokar AK, Djonin DV, Bhargava VK. Delay constrained rate and power adaptation over correlated fading channels. In: *IEEE Global Telecommunications Conference (GLOBECOM)*; 29 November–3 December 2004; Dallas, TX, USA. New York, NY, USA: IEEE. pp. 3448-3453.
- [14] Khoshnevis B, Khalaj BH. On a decentralized deterministic transmission power level selection algorithm in large aloha networks under saturation. In: *IEEE International Conference on Communications*; 11–15 June 2006; İstanbul, Turkey. New York, NY, USA: IEEE. pp. 5732-5737.
- [15] Gjendemsjo A, Oien GE, Orten P. Optimal discrete-level power control for adaptive coded modulation schemes with capacity-approaching component codes. In: *IEEE International Conference on Communications*; 11–15 June 2006; İstanbul, Turkey. New York, NY, USA: IEEE. pp. 5047-5052.
- [16] Srinivasa S, Jafar SA. Soft sensing and optimal power control for cognitive radio. *IEEE T Wirel Commun* 2010; 9: 3638-3649.

- [17] Noack A, Bok PB, Kruck S. Evaluating the impact of transmission power on QoS in wireless mesh networks. In: International Conference on Computer Communications and Networks (ICCCN); 31 July–4 August 2011; Maui, HI, USA. New York, NY, USA: IEEE. pp. 1-6.
- [18] Su W, Lee S, Pados DA, Matyjas JD. Optimal power assignment for minimizing the average total transmission power in hybrid-ARQ Rayleigh fading links. *IEEE T Commun* 2011; 59: 1867-1877.
- [19] Zou M, Chan S, Vu HL, Ping L. Throughput improvement of 802.11 networks via randomization of transmission power levels. *IEEE T Veh Technol* 2016; 65: 2703-2714.
- [20] Nar PC, Çayırıcı E. PCSMAC: A power controlled sensor-MAC protocol for wireless sensor networks. In: Proceedings of the Second European Workshop on Wireless Sensor Networks; 2 February 2005; İstanbul, Turkey. New York, NY, USA: IEEE. pp. 81-92.
- [21] Galluccio L, Leonardi A, Morabito G, Palazzo S. On the convenience of turning off the radio interface and using multiple transmission power levels in sensor networks applying geographical forwarding. In: International Symposium on Wireless Communication Systems; 6–8 September 2006; Valencia, Spain. New York, NY, USA: IEEE. pp. 88-92.
- [22] Natarajan A, Silva B, Yap KK, Motani M. Link layer behavior of body area networks at 2.4 GHz. In: International Conference on Mobile Computing and Networking; 20–25 September 2009; Beijing, China. New York, NY, USA: ACM. pp. 241-252.
- [23] Lee W, Choi M, Kim N. Experimental link channel characteristics in wireless body sensor systems. In: International Conference on Information Network; 1–3 February 2012; Bali, Indonesia. New York, NY, USA: IEEE. pp. 374-378.
- [24] Zogovic N, Dimic G, Bajic D. Packet length and transmission power adaptation for energy-efficiency in low-power wireless communications. In: International Conference on Telecommunication in Modern Satellite Cable and Broadcasting Services (TELSIKS); 5–8 October 2011; Nis, Serbia. New York, NY, USA: IEEE. pp. 497-500.
- [25] Farayev B, Sadi Y, Ergen SÇ. Optimal power control and rate adaptation for ultra-reliable M2M control applications. In: IEEE Globecom Workshops (GC Wkshps); 6–10 December 2015; San Diego, CA, USA. New York, NY, USA: IEEE. pp. 1-6.
- [26] Jouhari M, Ibrahim K, Benattou M. Topology control through depth adjustment and transmission power control for UWSN routing protocols. In: International Conference on Wireless Networks and Mobile Communications (WINCOM); 20–23 October 2015; Marrakesh, Morocco. New York, NY, USA: IEEE. pp. 1-5.
- [27] Liu CH, Rong B, Cui S. Optimal discrete power control in poisson-clustered ad hoc networks. *IEEE T Wirel Commun* 2015; 14: 138-151.
- [28] Sisodiya N, Shetty DP. Total power minimization using dual power assignment in wireless sensor networks. In: International Conference on Information Technology (ICIT); 21–23 December 2015; Bhubaneswar, India. New York, NY, USA: IEEE. pp. 26-30.
- [29] Zuniga M, Krishnamachari B. Analyzing the transitional region in low power wireless links. In: IEEE Communications Society Conference on Sensor and Ad Hoc Communications and Networks (SECON); 4–7 October 2004; Santa Clara, CA, USA. New York, NY, USA: IEEE. pp. 517-526.
- [30] Yetgin H, Cheung KTK, El-Hajjar M, Hanzo LH. A survey of network lifetime maximization techniques in wireless sensor networks. *IEEE Commun Surv Tut* 2017; 19: 828-854.
- [31] Lin S, Zhang J, Zhou G, Gu L, He T, Stankovic JA. ATPC: Adaptive transmission power control for wireless sensor networks. In: International Conference on Embedded Networked Sensor Systems (SenSys); 31 October–3 November 2006; Boulder, CO, USA. New York, NY, USA: ACM. pp. 223-236.